Optical Thomson Scattering Measurements of Plasma Parameters in the Ablation Stage of Wire Array *Z* Pinches

A. J. Harvey-Thompson,[1,*] S. V. Lebedev,[1] S. Patankar,[1] S. N. Bland,[1] G. Burdiak,[1] J. P. Chittenden,[1] A. Colaitis,[1] P. De Grouchy,[1] H. W. Doyle,[1] G. N. Hall,[1] E. Khoory,[1] M. Hohenberger,[2] L. Pickworth,[1] F. Suzuki-Vidal,[1] R. A. Smith,[1] J. Skidmore,[1] L. Suttle,[1] and G. F. Swadling[1]

[1]*Blackett Laboratory, Imperial College, London, SW7 2BW, United Kingdom*

[2]*Department of Mechanical Engineering, University of Rochester, Rochester, New York 14627, USA*

(Received 20 October 2011; published 3 April 2012)

A Thomson scattering diagnostic has been used to measure the parameters of cylindrical wire array *Z* pinch plasmas during the ablation phase. The scattering operates in the collective regime ($\alpha > 1$) allowing spatially localized measurements of the ion or electron plasma temperatures and of the plasma bulk velocity. The ablation flow is found to accelerate towards the axis reaching peak velocities of 1.2–1.3×10^7 cm/s in aluminium and $\sim 1 \times 10^7$ cm/s in tungsten arrays. Precursor ion temperature measurements made shortly after formation are found to correspond to the kinetic energy of the converging ablation flow.

DOI: 10.1103/PhysRevLett.108.145002 PACS numbers: 52.59.Qy, 52.25.Os

Wire array *Z* pinch implosions can efficiently convert stored electrical energy into powerful bursts of soft x rays. Experiments on the 20 MA *Z* pulsed power generator [1] have achieved peak powers of 280–300 TW with a >2 MJ yield at 20% efficiency [2] by imploding cylindrical arrays consisting of hundreds of fine metallic wires. It was found [3–5] that in wire array *Z* pinches, the wires remain stationary for the first 60%–80% of the implosion time and steadily ablate plasma which is accelerated by the $\mathbf{j} \times \mathbf{B}$ force. This ablation flow distributes mass in the array interior which sets the initial conditions for the implosion phase. The ablation mass distribution depends on the ablation rate, dm/dt, and on the flow velocity, which are related via force—momentum balance. However, the flow velocity was not measured in past experiments apart from the velocity of the initial part of the flow which was inferred from the time of plasma appearance on the array axis and from endon interferometry measurements, giving $V \sim 1.5 \times 10^7$ cm/s [6,7]. The velocity of the ablation flow in the later stages, when the majority of the ablated material is moving into the array interior, is not known. Instead, the ablation rate and mass redistribution is often discussed using the so-called ''ablation velocity'', introduced in the rocket model [3] via momentum balance arguments, which is inferred from the implosion dynamics or from unfolds of x-ray radiography measurements of mass distribution in the array interior [3,4,8,9].

Numerical simulations [10,11] show that velocity is changing both with time and with the radial position of the flow, indicating that the flow is accelerated by the $\mathbf{j} \times \mathbf{B}$ force acting on the plasma in the array interior. However, these simulations do not model the initial heating of the wires and the process of conversion of initially cold metallic wires into a plasma. Instead, simulations start from wire material already converted into plasma at some initial temperature and density, and these initial conditions are adjusted to produce agreement of the simulated implosion dynamics with experimental observations. Direct measurements of the ablation flow velocity and density are needed to allow verification of these numerical models. Knowledge of the flow velocity is also important for other applications of different wire array *Z* pinch configurations, used, e.g., in laboratory astrophysics [12] and other high energy density physics basic science research.

In this Letter, we present the first measurements of the ablation plasma flow velocities in Al and W cylindrical wire array *Z* pinches. The measurements were obtained using an optical Thomson scattering diagnostic working in the collective scattering regime [13]. The Doppler shift of the ion feature in the scattered spectrum allowed measurements of the flow velocity of the ablated plasma while the shape of the spectrum provided measurements of the ion (T_i) and electron (T_e) temperatures of the plasma [13]. The measured radial velocity profiles show that the plasma flow undergoes additional acceleration inside the arrays, consistent with the presence of current and magnetic fields in the array interior [14]. The peak velocities in the ablation flows are similar for Al and W wire arrays, reaching $\sim 1.2 \times 10^7$ cm/s and $\sim 1 \times 10^7$ cm/s, respectively. The high ion temperatures of the precursor plasma accumulating on the array axis, measured at the time of the first plasma arrival at the array axis, are consistent with the kinetic energy of the ions in the ablation flow. Comparisons of the experimental results with 3D MHD simulations using the code GORGON show a good agreement for Al wire arrays and considerable differences for W wire arrays at early times, due to the low collisionality of energetic *W* ions which the code does not model.

Experiments were performed on the MAGPIE generator [15] (1.4 MA, 250 ns) using a frequency doubled Nd-YAG

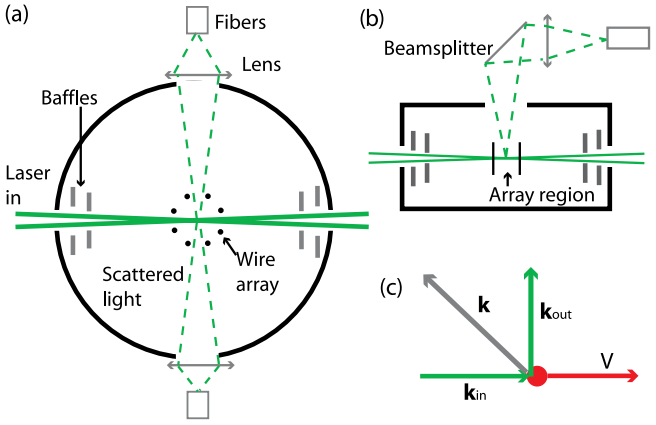

FIG. 1 (color online). (a) Diagram of the setup used for side-on collection and (b) endon collection of scattered light. (c) The scattering geometry used in experiments.

laser (~ 3 J, 8 ns, 532 nm) for the Thomson scattering diagnostic. Cylindrical arrays of 16 mm diameter with 8, 16, or 32 Al or W wires were used. A schematic of the experimental setup is shown in Fig. 1(a). The laser is focused into the chamber using an $f = 2.5$ m lens giving a ~ 500 μm spot diameter that remains approximately constant as the beam passes through the array. Light scattered from the plasma is collected by $f/10$ lenses placed 90° to the input beam either to the side or above the chamber [Figs. 1(a) and 1(b), respectively] and is imaged onto the input of the optic fiber bundles. The frequency shift of the observed scattered light due to the plasma motion is given by $\Delta\omega = \mathbf{k} \cdot \mathbf{V}$, where $\mathbf{k} = \mathbf{k}_{\text{out}} - \mathbf{k}_{\text{in}}$ as shown in Fig. 1(c). The output of the optical fibers are connected to a 0.5 m imaging ANDOR spectrometer with a 2400 lines/mm grating giving a spectral resolution of 0.25 Å or 0.45 Å (defined as being the standard deviation, σ, of the Gaussian used to fit the spectrum), determined by the diameter of the fibers in the bundles used. The spectrum is recorded using an ANDOR ICCD camera with a 4 ns gate time synchronized with the laser pulse.

An alignment pin, installed and removed under vacuum is used to align the positions of the fiber bundles and record the unshifted spectrum [Fig. 2(a)]. In most cases the fiber bundles used to collect scattered light consisted of a linear array of 7, 200 μm diameter fibers spaced 490 μm apart along a line. Light scattered from the plasma is focused onto the fibers, thus providing in a single shot, measurements of the scattering spectra from several spatial positions along the laser beam at a separation determined by the fiber spacing and the magnification of the setup.

Figure 2(b) shows the scattered signal from the ablation flow of a 32×10 μm W array at 155 ns after current start. The laser enters the array between two wires and passes through the array axis [Fig. 1(a)] so scattering is observed from ablated plasma located between the wires. At this time the array wires remain at their original positions as dense wire cores surrounded by a coronal plasma. The wire cores obstruct the line of sight through the side of the array, restricting the number of scattering positions from which the side-on registration is possible. Therefore the scattered light is collected by a fiber bundle located above the array, as shown in Fig. 1(b), looking down through the open electrode of the array. Measurements of the scattered spectrum with a spectral resolution of 0.45 Å, are obtained from seven regularly spaced positions spanning 7.8 mm along the array diameter. Each fiber collected scattered light from a 700 μm diameter spot, which determined the spatial resolution. The fibers typically covered positions between $r = 6.5$ mm and $r = -1.3$ mm, including the on-axis precursor. The data are analyzed by averaging the intensity of the central region in each spectrum over 11 pixels of the camera output in the direction perpendicular to the spectral

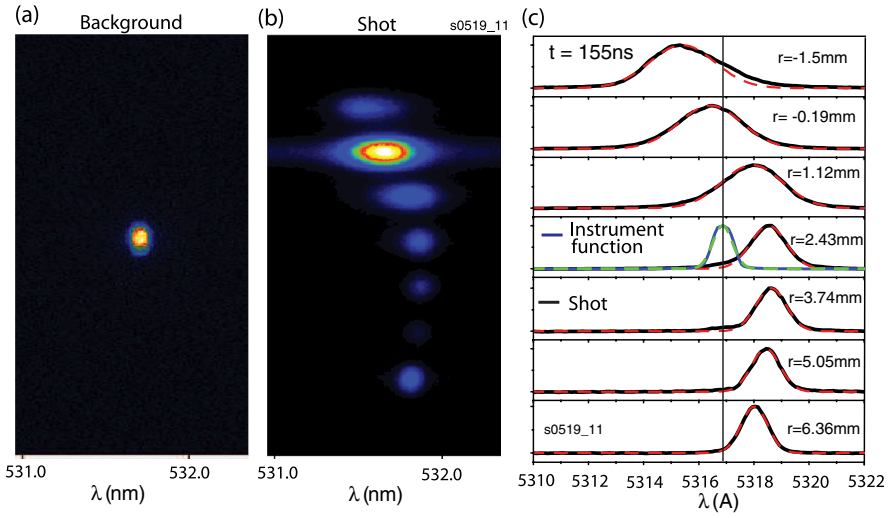

FIG. 2 (color online). (a) The output spectrum from laser light scattered from an alignment pin into the 7 fiber bundle and (b) from the ablation flow in a 32 wire W array during the shot. Lineouts of these spectra with Gaussian fits are shown in (c).

dispersion to improve the signal to noise ratio, giving the spectra shown in Fig. 2(c). Each spectrum represents the so-called ion feature in the collective scattering signal [13]. In the ablation flow from W wires the ion feature has a single peak whose width is dependent on T_i and also on the spread of the flow velocities inside the scattering volume. The scattering spectra are shifted from the laser wavelength by the motion of the plasma, and the shift is proportional to the flow velocity. This shift is measured by comparing the shot spectrum to that from the alignment pin. The error in the mean wavelength shift can be determined to an accuracy of ± 0.04 Å, giving an error in the velocity of $\pm 1.5 \times 10^5$ cm/s. Additional errors arise from the range of scattering $\mathbf{k}$ vectors collected by the fibers ($\Delta\mathbf{k}/\mathbf{k} = 0.025$) and from the measurements of the scattering angle ($\pm 3°$). The total error in the velocity measurements is estimated to be $\pm 4 \times 10^5$ cm/s ($\sim 4\%$).

The measured radial velocity profiles of the ablation flow in Al and W arrays are shown in Figs. 3(a) and 3(b), respectively, along with profiles simulated using the 3D MHD code GORGON [16,17]. The velocity profiles of Al arrays were taken with the probing laser beam propagating between the wires for both 16 and 32 wire arrays. In all the measurements it was found that plasma ablated from the wires is accelerated towards the axis, reaching a peak velocity of $1.2–1.3 \times 10^7$ cm/s near the axis, indicating the presence of current in the ablated plasma. The velocity profiles for 16 and 32 wire arrays at similar times are closely matched suggesting little dependence on wire number. The profiles at different times are also similar, although the velocity is slightly higher close to the wires at the later time. As the plasma reaches the axis it decelerates, colliding with plasma streams from the other wires and with plasma already accumulated on axis in the precursor column [7]. The simulated Al velocity profile agrees very well with the data matching the absolute values of velocity and the acceleration towards the axis.

The velocity profiles measured in the W arrays are qualitatively similar to those in Al arrays. The plasma accelerates from the outer radius towards the axis reaching a peak velocity of $\sim 1 \times 10^7$ cm/s before being decelerated by the precursor plasma. One of the presented velocity profiles was obtained for a wire array consisting of 31 equally spaced W wires. In this case, the laser beam entered between two wires, passed through the low density precursor on the array axis and focused onto a wire at the opposite side of the array. This allowed a direct measurement of the velocity of the plasma directly emanating from the wire by collecting light from several positions between that wire and the array axis. A comparison of measurements between this configuration and those taken for scattering volumes between the wires (32 wire case) shows essentially no difference in the flow velocity between the two cases.

The simulated velocity profiles deviate significantly from these experimental results. The simulations predict a higher velocity at 150 ns, reaching a maximum of $\sim 1.7 \times 10^7$ cm/s, before dropping later in time to $\sim 1.3 \times 10^7$ cm/s. The biggest difference between the simulated and measured velocity profiles for W is in how the velocity reduces as the flow approaches the axis. It is seen in Fig. 3(b) that for early times ($\sim$150 ns), the velocity reduces at $r \sim 1$ mm by almost a factor of 2, while in the simulations it continues to rise until $r \sim 0.2$ mm, the radius of the precursor column. The observed difference is due to the lower collisionality of W ions at early stages producing a broad precursor column [3,7], which is not modeled by MHD codes. This effect is much stronger in W due to the high kinetic energy of the W ions (9.6 keV versus 2 keV for Al). The corresponding ion-ion mean free paths describing the scattering of the streams are $\sim$6 mm for W and $\sim$0.4 mm for Al (using $n_e = (0.5 \text{ or } 2) \times 10^{18}$ cm^{-3} measured by interferometry and $Z = 7$ or 4 from the simulations for W and Al, respectively). Previous experimental investigations and hybrid particle in cell simulations [7,18] show that for W arrays at our experimental conditions the onset of collisionality and the formation of a dense, narrow precursor is delayed by $\sim$50–70 ns from the time of the first arrival of plasma at the axis.

The deceleration of the inward plasma flow near the array axis measured in W wire arrays [Fig. 3(b)], is accompanied by an increase in the spectral width of the

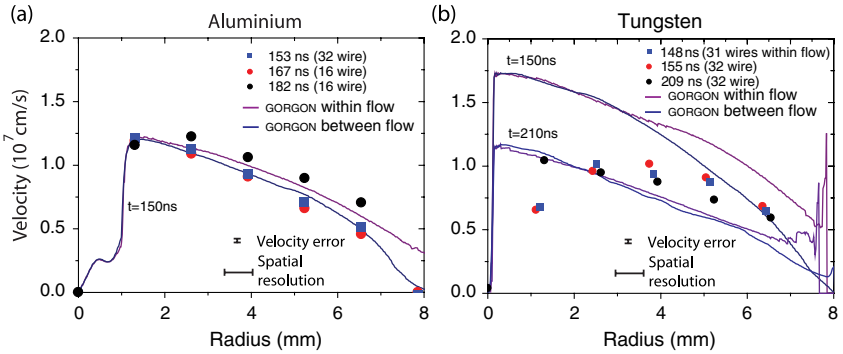

FIG. 3 (color online). The radial velocity profile for Al arrays (a) and W arrays (b) with simulated profiles from GORGON. The profiles were taken looking between wires apart from the 31 wire W array looking directly into a wire.

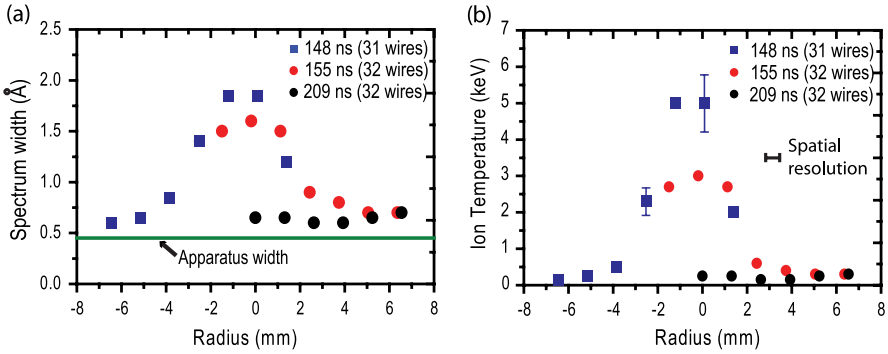

FIG. 4 (color online). The spectral width (a) and the corresponding ion temperature (b) of the ablation flow plasma in W arrays taken from the same spectra as the flow velocity profiles in Fig. 3(b).

scattered signal as seen in Fig. 2. It is seen in Fig. 4(a) that at small radii the width increases to 1.5–2 Å, significantly exceeding the resolution (apparatus width) of the registration system (0.45 Å for the used fiber bundle). This increase can be interpreted as an increase of the ion temperature due to thermalization of the kinetic energy of W ions in the flow. Figure 4(b) shows radial profiles of the ion temperature, determined by fitting a theoretical scattered spectrum [13] convolved with the apparatus function of the spectrometer. It is seen that at early times ($\sim$150 ns) the ion temperature near the array axis is $\sim$5 keV. Later in time at $\sim$209 ns, the spectral width of the scattered signal and thus the temperature remains small at all radii. This time corresponds to the stage when a narrow precursor plasma column is formed following a rapid cooling of the plasma due to ionization and radiation energy losses as discussed in [3,7].

The scattering spectra from the precursor plasma accumulated on the axis of the array can provide information on the evolution of the temperature of this plasma and also additional information about the velocity of the ablated plasma flow. The latter is particularly important for early time measurements, when the density of the ablated plasma away from the axis is too small for light scattered away from the array axis to be registered. The typical scattering spectra from W and Al precursors obtained at different times are shown in Fig. 5. The scattered light in these measurements was collected in the side-on setup shown in Fig. 1(a) and a circular-to-rectangular fiber bundle made of 100 μm diameter fibers was used to improve the spectral resolution to 0.25 Å [Fig. 5(d)].

Figure 5(a) shows the scattered spectrum from a W precursor at 100 ns, shortly after the first plasma is detectable on the array axis. The scattering spectrum has

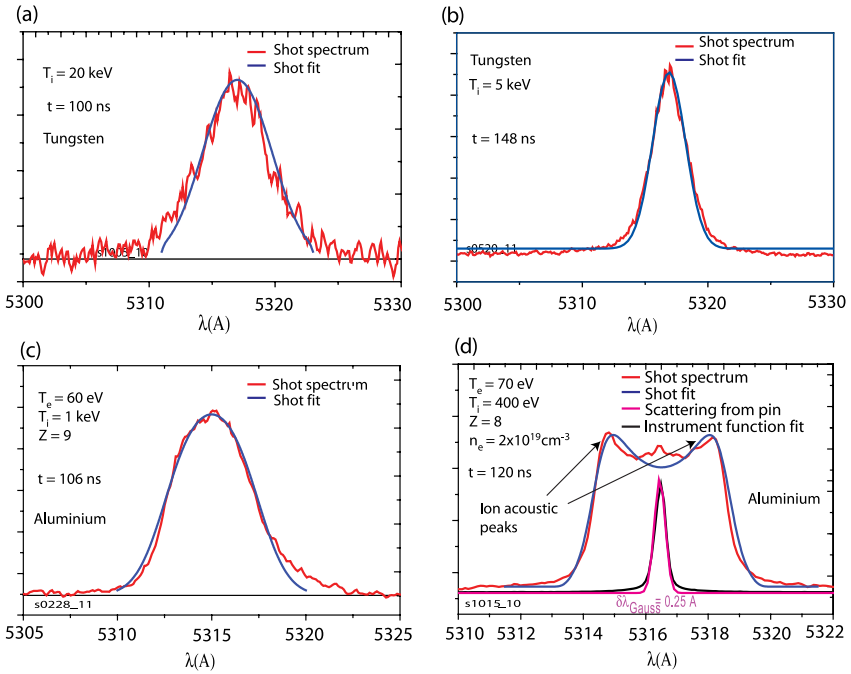

FIG. 5 (color online). Thomson scattering spectra from precursor plasmas in W wire arrays (a) and (b), and in Al wire arrays (c) and (d).

a broad Gaussian-like shape with a spectral width of ~4 Å. The presence of a single peak suggests that $T_i > ZT_e$ in the plasma [13], a result of the high kinetic energy of the W ions in the ablation flow. The theoretical fit to the spectrum gives $T_i = 20 \pm 5$ keV. Were the kinetic energy of the ablation flow travelling at the velocity measured by Thomson scattering at later times ($\sim 1 \times 10^7$ cm/s) to be thermalized completely without loss, a temperature of only 6.4 keV would be expected. The significantly higher precursor ion temperature indicates a higher flow velocity of the streams arriving on axis at early times, requiring an ion kinetic energy of 30 keV for a 20 keV ion temperature (assuming $E_{\text{ion}} = \frac{3}{2}\kappa T_{\text{ion}}$) corresponding to a velocity of $V = 1.75 \pm 0.22 \times 10^7$ cm/s. This is closer to the velocity of 1.5×10^7 cm/s which was previously found from the endon measurements [6] of the motion of the first plasma ablated from the wires. This suggests that there is a decrease of the flow velocity with time at the beginning of the ablation phase, similar to what is seen in simulations (Fig. 2), but occurring earlier in time. The scattering spectrum measured for the W precursor plasma later at 148 ns [Fig. 5(b)] gives $T_i = 5 \pm 0.8$ keV, which is consistent with the expected 6.4 keV temperature from a thermalization of the kinetic energy of W ions moving with the measured flow velocity of 1×10^7 cm/s.

Figures 5(c) and 5(d) show the scattered spectra from an Al precursor at 106 ns and 120 ns, respectively. At 106 ns, the Al precursor plasma column has just formed and the ion temperature of $T_i = 1 \pm 0.15$ keV measured from this spectrum requires an ablation flow velocity of $V = 0.98 \pm 0.08 \times 10^7$ cm/s, just below the measured flow velocity of $1.2–1.3 \times 10^7$ cm/s in Fig. 3(a).

With time, the ion temperature of the Al precursor should decrease due to energy transfer to the electrons, radiative cooling, and ionization losses, and this is confirmed by the changing shape of the scattering spectra at later times. The spectrum measured at 120 ns [Fig. 5(d)] has two ion acoustic peaks which appear when the value of ZT_e becomes larger than T_i. The separation of the two peaks is related to ZT_e, while their width is determined by T_i [13]. The theoretical fit to the spectrum gives $T_i = 400 \pm 50$ eV and $T_e = 70 \pm 8$ eV with $Z = 8$. The origin of the central peak in the spectrum, at the laser wavelength, needs to be investigated but is unlikely to be due to stray laser light in the system.

In conclusion, Thomson scattering measurements show that the ablation plasma flow undergoes additional acceleration inside the array reaching a peak velocity of $1.2–1.3 \times 10^7$ cm/s in Al and $\sim 1 \times 10^7$ cm/s in W. This is well reproduced by MHD simulations of collisional flow, such as in Al arrays, but deviates significantly for the collisionless W plasma flow at early times. The found discrepancy highlights the need for further improvements in the computational models used. Temperature profiles show that the ablation flow is initially thermalized with little loss producing ion temperatures in the precursor plasma of 20 keV and 1 keV at 100 ns in W and Al, respectively.

The authors are grateful to Dr. A. D. Heathcote for many useful discussions. This research was sponsored by the EPSRC Grant No. EP/G001324/1, and by the DOE under Cooperative Agreements DE-F03-02NA00057 and DE-SC-0001063.

*Current address: Sandia National Laboratories, Albuquerque, New Mexico 87185, USA.

[1] R. B. Spielman *et al.*, Phys. Plasmas **5**, 2105 (1998).
[2] C. Deeney, M. R. Douglas, R. B. Spielman, T. J. Nash, D. L. Peterson, P. L'Eplattenier†, G. A. Chandler, J. F. Seamen, and K. W. Struve, Phys. Rev. Lett. **81**, 4883 (1998).
[3] S. V. Lebedev, F. N. Beg, S. N. Bland, J. P. Chittenden, A. E. Dangor, M. G. Haines, K. H. Kwek, S. A. Pikuz, and T. A. Shelkovenko, Phys. Plasmas **8**, 3734 (2001).
[4] M. E. Cuneo *et al.*, Phys. Rev. E **71**, 046406 (2005).
[5] V. V. Aleksandrov *et al.*, Plasma Phys. Rep. **27**, 89 (2001).
[6] S. V. Lebedev, R. Aliaga-Rossel, S. N. Bland, J. P. Chittenden, A. E. Dangor, M. G. Haines, and I. H. Mitchell, Phys. Plasmas **6**, 2016 (1999).
[7] S. C. Bott *et al.*, Phys. Rev. E **74**, 046403 (2006).
[8] D. B. Sinars, M. E. Cuneo, E. P. Yu, S. V. Lebedev, K. R. Cochrane, B. Jones, J. J. MacFarlane, T. A. Mehlhorn, J. L. Porter, and D. F. Wenger, Phys. Plasmas **13**, 042704 (2006).
[9] S. V. Lebedev, D. J. Ampleford, S. N. Bland, S. C. Bott, J. P. Chittenden, C. Jennings, M. G. Haines, J. B. A. Palmer, and J. Rapley, Nucl. Fusion **44**, S215 (2004).
[10] J. C. Chittenden, S. V. Lebedev, B. V. Oliver, E. P. Yu, and M. E. Cuneo, Phys. Plasmas **11**, 1118 (2004).
[11] E. P. Yu, B. V. Oliver, D. B. Sinars, T. A. Mehlhorn, M. E. Cuneo, P. V. Sasorov, M. G. Haines, and S. V. Lebedev, Phys. Plasmas **14**, 022705 (2007).
[12] B. A. Remington, R. P. Drake, and D. D. Ryutov, Rev. Mod. Phys. **78**, 755 (2006).
[13] J. Sheffield *et al.*, *Plasma Scattering of Electromagnetic Radiation* (Academic Press, New York, 1975).
[14] Magnetic fields in wire arrays were measured by V. V. Aleksandrov *et al.*, in *Dense Z-Pinches: 6th International Conference on Dense Z Pinches*, edited by J. C. Chittenden, AIP Conf. Proc. No. 808 (AIP, New York, 2006), p. 3; and by J. B. Greenly, M. Martin, I. Blesener, D. Chalenski, P. Knapp, and R. McBride, in *Dense Z-Pinches: 7th International Conference on Dense Z Pinches*, edited by D. A. Hammer, AIP Conf. Proc. No. 1088 (AIP, New York, 2009), p. 53.
[15] I. H. Mitchell, J. M. Bayley, J. P. Chittenden, J. F. Worley, A. E. Dangor, and M. G. Haines, Rev. Sci. Instrum. **67**, 1533 (1996).
[16] J. P. Chittenden and C. J. Jennings, Plasma Phys. Controlled Fusion **46**, B457 (2004).
[17] A. Ciardi *et al.*, Phys. Plasmas **14**, 056501 (2007).
[18] M. Sherlock, J. P. Chittenden, S. V. Lebedev, and M. G. Haines, Phys. Plasmas **11**, 1609 (2004).